

# Chapter 6

## A Multi-Signal Variant for the GPU-Based Parallelization of Growing Self-Organizing Networks

Giacomo Parigi, Angelo Stramieri, Danilo Pau and Marco Piastra

**Abstract** Among the many possible approaches for the parallelization of self-organizing networks, and in particular of *growing* self-organizing networks, perhaps the most common one is producing an optimized, parallel implementation of the standard sequential algorithms reported in the literature. In this chapter we explore an alternative approach, based on a new algorithm variant specifically designed to match the features of the large-scale, fine-grained parallelism of GPUs, in which multiple input signals are processed at once. Comparative tests have been performed, using both parallel and sequential implementations of the new algorithm variant, in particular for a growing self-organizing network that reconstructs surfaces from point clouds. The experimental results show that this approach allows harnessing in a more effective way the intrinsic parallelism that the self-organizing networks algorithms seem intuitively to suggest, obtaining better performances even with networks of smaller size.

**Keywords** Growing self-organizing networks · Graphics processing unit · Parallelism · Surface reconstruction · Topology preservation

### 6.1 Introduction

From a general point of view a self-organizing network is composed by units that adapt themselves, through limited and local interactions, to input signals from some predefined space. In most cases a topology is defined among these units by a set of

---

G. Parigi (✉) · A. Stramieri · M. Piastra  
Computer Vision and Multimedia Lab, University of Pavia, Via Ferrata 1, 27100 Pavia, PV, Italy  
e-mail: giacomo.parigi@gmail.com

D. Pau  
Advanced System Technology, STMicroelectronics, Via Olivetti 2,  
20864 Agrate Brianza, MB, Italy

binary connections. At first sight, the adaptation process may look inherently parallel, since each unit follows the same predetermined behavior and in many cases, as long as two units are sufficiently far away in the network, they do not interact in any way.

Nonetheless, most of the algorithms in the literature are described as sequential procedures, in the sense that input signals are submitted one by one to the network and processed each in a sequential way. This means that, in most cases, also units will be adapted sequentially, one after the other, even when they can be considered as mutually independent, i.e. with input signals that are sufficiently distant in the input space.

In a typical algorithm, each input signal has to be compared to all units in the network, in order to find the closest one and adapt the latter and its neighbors to the input signal. For reasons that will be described in detail later on, this operation is dominant in terms of execution time, and is therefore the obvious focus for parallel implementation. In this respect, two main methods emerge: *data partitioning* methods, in which the input signals are partitioned across parallel tasks, whereby each task involves the entire network and processes just one input signal; *network partitioning* methods, in which the units of the network are partitioned across parallel tasks, whereby each task considers all input signals but only in relation to the units belonging to its partition. These two approaches are thoroughly examined in [2] for the parallelization of Kohonen’s self-organizing map [3]. In particular, in the former work, a data partitioning approach is described for the batch version of the algorithm, and a network partitioning approach for the on-line version of the algorithm, in both cases for an SP2 parallel computer.

As a matter of fact, perhaps the most common approach for the parallel implementation of self-organizing networks described in the literature (see for instance [4–7]), is to adapt the network-partitioning method to the standard, sequential version of the algorithm.

In an effort to better harness the “latent parallelism” of self-organizing networks, a new algorithm variant for *growing* self-organizing networks is proposed in this chapter. In this *multi-signal* algorithm variant, a number of signals are submitted to the network and elaborated at once during each iteration. This variant is explicitly intended for a data-partitioning approach to parallelization, which, as described in [2], may offer “the potential for much greater scalability, since the parallel granularity is determined by the volume of data, which is potentially very large”. In particular the new algorithm focuses on *growing* self-organizing networks and this entails dealing with some further functional aspects, that are not present in the algorithm for self-organizing maps considered in [2]. This aspect will be described in Sect. 6.2.

The new multi-signal algorithm has been designed to match the features of the large-scale, fine-grained parallelism of GPUs (Graphics Processing Units). Beside its computational capabilities, this hardware has gained a large popularity due to the lower costs compared to those of more traditional high-performance computing solutions. For instance, in [8], GPUs have been defined “probably today’s most powerful computational hardware for the dollar”.

The GPU-based implementation of the multi-signal variant, has shown good performances in all the tests performed, reaching noticeable speed-ups even for smaller

networks. In addition, the new multi-signal algorithm has shown some interesting differences w.r.t. the standard single-signal algorithm: in the tests performed, the multi-signal algorithm always required less input signals to reach termination than the single-signal counterpart. These aspects will be further discussed in Sect. 6.3.

## 6.2 Methods

### 6.2.1 Growing Self-Organizing Networks

In the discussion that follows, we consider as reference a network in which each unit is associated to a *reference vector* in the input space, and a topology is defined by a set of binary connections between the units. These connections also define the local topology, or *neighborhood*, of each unit. In a self-organizing network units are progressively adapted during the learning process. In addition, *growing* self-organizing networks, like GNG [9], GWR [10] and SOAM [1] have the following characteristics:

- during the learning process the number of units varies, and can both grow and shrink;
- the topology of connections between units varies as well, since connections are both created and destroyed during the learning process.

In general, the learning process of a growing self-organizing network can be described as a basic iteration, which is repeated until some convergence criterion is met:

#### 1. *Sample*

Generate at random one input signal  $\xi$  with probability  $P(\xi)$ . Usually the support of  $P(\xi)$  coincide with the *region of interest*, i.e. the region of input space to be considered.

#### 2. *Find Winners*

Compute the distances  $\|\xi - \mathbf{w}_i\|$  between each reference vector and the input signal and find the  $k$ -nearest units. In most cases  $k = 2$ , i.e. the nearest (*winner*) and second-nearest units are searched for.

#### 3. *Update the Network*

Create a new connection between the winner and the second-nearest unit, if not existing, or reset the existing one.<sup>1</sup>

Adapt the reference vector of the winner unit and of its topological neighbors, with a law of the type:

$$\begin{aligned}\Delta \mathbf{w}_b &= \varepsilon_b \|\xi - \mathbf{w}_b\|, \\ \Delta \mathbf{w}_i &= \varepsilon_i \eta(i, b) \|\xi - \mathbf{w}_i\|,\end{aligned}\tag{6.1}$$

---

<sup>1</sup> An *aging* mechanism is also applied to connections (see for instance [9]).

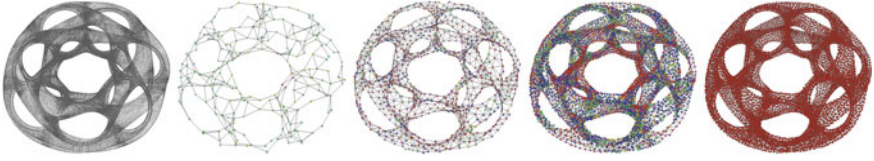


**Fig. 6.1** The SOAM [1] reconstructs a surface from the point cloud on *left*. At the end, all units converge to the same stable state

where  $\mathbf{w}_b$  is the reference vector of the winner and  $\mathbf{w}_i$  are the reference vectors of the neighboring units.  $\varepsilon_b, \varepsilon_i \in [0, 1]$  are the *learning rates*, with  $\varepsilon_b \gg \varepsilon_i$ . The function  $\eta(i, b) \leq 1$  determines how neighboring units are adapted. In most cases  $\eta(i, b) = 1$  if units  $b$  and  $i$  are connected and 0 otherwise. During this phase, new units can be created and old units can be removed, with methods that may vary depending on the specific algorithm.

The three steps above are iterated until some convergence criterion is met: typically, in most self-organizing networks, including growing ones, this criterion is a threshold on the overall quantization error, i.e. the mean squared distance between input signals and the corresponding winners. For the purposes of this work we adopted the SOAM algorithm, that has a termination criterion which does not depend on a threshold. In the SOAM algorithm, in fact, the learning process terminates when all units have reached a local topology consistent with that of a surface and therefore the network represents the triangulation of the surface that has to be reconstructed from input signals (see Fig. 6.1). The clear termination criterion in the SOAM algorithm is fundamental for comparing the performances and the different behaviors of the two variants of the algorithm, i.e. single-signal and multi-signal, and their implementations.

The methods adopted for adding and removing units during the *Update* phase greatly vary depending on the algorithm. In GNG, for example, new units are inserted at regular intervals, in the neighborhood of the unit  $i$  that has accumulated the largest mean squared error. In contrast, in GWR new units are added whenever the distance between the winner unit and the input signal  $\xi$  is greater than a predefined *insertion threshold*. The new unit is positioned in proximity of the winner and the network topology is updated. The SOAM algorithm is similar to the GWR, with the difference that the insertion threshold may vary during the learning process, in order to reflect the *local feature size* (LFS) of the surface being reconstructed (see Sect. 6.3.1).

In terms of time complexity, the *Find Winners* phase is dominant in general. In fact, assuming that the number  $k$  of nearest neighbors is constant and small, the *Find Winners* phase has  $\mathcal{O}(N)$  time complexity, where  $N$  is the total number of units. Although the complexity of the *Update* phase may greatly vary depending on how the function is defined (see for instance the Neural Gas algorithm [11]), as a matter of fact in most growing self-organizing networks, including the SOAM algorithm, this update is local and limited to the connected neighbors of the winner, so that the *Update* phase can be assumed to have  $\mathcal{O}(1)$  time complexity. Furthermore, in this

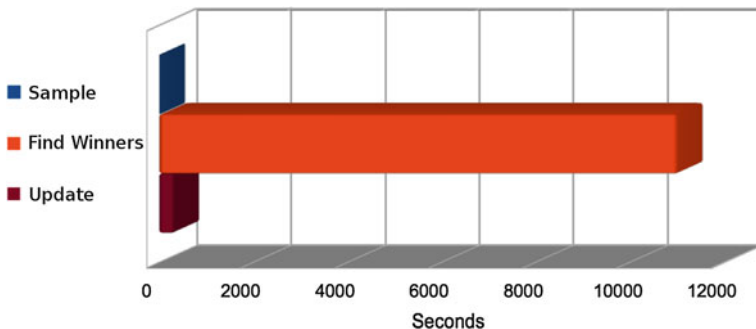


**Fig. 6.2** Single-phase time to convergence of the SOAM algorithm (average values on the whole test set)

discussion, we will not consider the *Sample* phase in detail: sampling methods, in fact, are application-dependent and not necessarily under the control of the algorithm.

The dominance of the *Find Winners* phase in terms of time complexity is confirmed by experiments. The graph in Fig. 6.2 shows the mean values obtained from the experiments described in Sect. 6.3. These results are in line with the ones reported in the literature (see for example [4] for a detailed analysis), in that the percentage of the execution time spent in the *Find Winners* phase remains as low as 50–60% of the total execution time as long as the network remains small (i.e. 250–500 units), but grows rapidly to 95% and more as the network size increases and more signals are processed.

## 6.2.2 The Multi-Signal Variant

In the *multi-signal* variant proposed here, at each iteration  $m \gg 1$  signals are considered at once. The basic iteration hence becomes:

### 1. *Sample*

Generate at random  $m$  input signals  $\xi_1, \dots, \xi_m$  according to the probability distribution  $P(\xi)$ , as described before.

### 2. *Find Winners*

For each signal  $\xi_j$ , compute the distances  $\|\xi_j - \mathbf{w}_i\|$  between each reference vector and the input signal and find the  $k$ -nearest units.

### 3. *Update the Network*

For each signal  $\xi_j$ , perform the update operations specified in the previous section.

The first two phases in the above iteration pose no particular problems, since all the involved operations performed for each signal are mutually independent. In contrast, during the *Update* phase, the operations performed for different signals may collide. In particular three kinds of collision can occur:

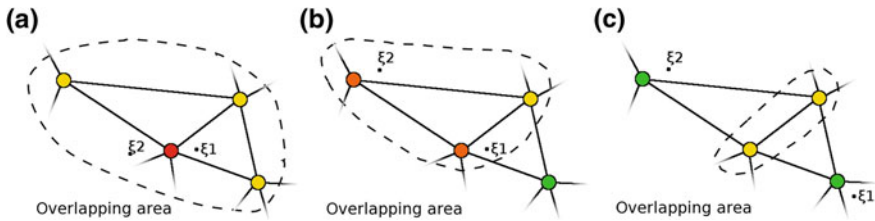


**Fig. 6.3** Collision caused by two different input signals  $\xi_1$  and  $\xi_2$ . In (a) the two signals share the same winner, hence all direct neighbors. In (b) and (c) the winner is different, but the neighbors are shared. All three cases would lead to colliding adaptations

**Adapt Position.** Two or more signals lead to the adaptation of the same unit in the network. Collisions of this kind are usually not isolated, since the collision can happen both for the winner and for the neighboring units, as described in Fig. 6.3.

**Modify Neighborhood.** Two or more signals lead to modifying the neighborhood of the same unit. This may be caused by either the insertion/removal of units or the creation/removal of edges.

**Insert Edge.** Two or more signals lead to the insertion of the same edge.

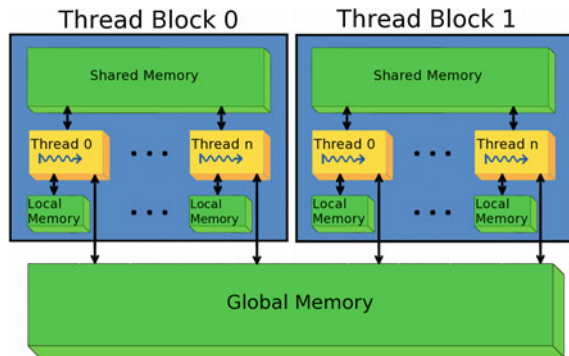
In the multi-signal variant presented here, the main concern in choosing the method for managing the above collisions is maintaining a coherent behavior with respect to the single-signal algorithm, and allow an unbiased comparison of the performances. At the same time, the method must be simple enough. The solution adopted is using an implicit *lock* on the winner unit: no two or more input signals having the same winner can cause any of the colliding modifications to be performed, as only the first incoming signal, in a random order, will produce the corresponding effect, while other signals for the same winner will just be *discarded*.

Collisions apart, the behavior of the new variant is *different* from the original, single-signal algorithm. In the experiments described in Sect. 6.3, in fact, the multi-signal variant always required a smaller number of signals to reach convergence, regardless of the implementation. This aspect will be discussed in more detail in Sect. 6.3.2.

### 6.2.3 Graphics Processing Units

Graphics Processing Units (GPUs) are specialized and optimized for graphic applications, and are typically mounted on dedicated boards with private onboard memories. During these last years, GPUs have evolved into general-purpose parallel execution machines [12]. Until not many years ago, in fact, the only available programming interfaces (API) for GPUs were very specific, forcing the programmer to translate the task into the graphic primitives provided. Gradually, many general-purpose API for parallel computing have emerged, which are suitable for GPUs as well. This set

**Fig. 6.4** Standard GPU memory hierarchy



of API includes, for instance, RapidMind [13], PeakStream [14] or the programming systems owned by NVIDIA and AMD, respectively CUDA (Compute Unified Device Architecture) [15] and CTM (Close to Metal) [16], together with proposed vendor-independent standards like OpenCL [17].

Albeit with some differences, all these API adopt the general model of *stream computing*: data elements are organized in *streams*, which are ordered sets of data; a set of streams is processed by the same *kernel*, intended as a set of functions to be computed in parallel, and produces another set of streams as output. Each kernel is executed on a set of GPU cores in the form of concurrent *threads*, each executing the same program on a different stream of data. Within a kernel, threads are grouped into blocks and each block is executed in sync. In case of branching of the execution, the block is partitioned in two: all the threads on the first branch are executed in parallel and then the same is done for all the threads in the second branch. This general model of parallel execution is often called SIMT (single-instruction multiple-thread) or SPMD (single-program multiple-data); compared to the older SIMD, it allows greater flexibility in the flow of different threads, although at the cost of a certain degree of serialization, depending on the program. This means that, although independent thread executions are possible, blocks of coherent threads with limited branching will make better use of the GPU's hardware.

In typical GPU architectures, onboard and on-chip memories are organized in a hierarchy (Fig. 6.4): *global* memory, i.e. accessible by all threads in execution, *shared* memory, i.e. a faster cache memory dedicated to each single thread block and *local* memory and/or registers, which are private to each thread.

Another noteworthy feature of modern GPUs is the wide-bandwidth access to onboard memory, on the order of 10x the memory access bandwidth on typical PC platforms. To achieve best performances, however, memory accesses by different threads should be made aligned and coherent, in order to *coalesce* them into fewer, parallel accesses addressing larger blocks of memory. Incoherent accesses, on the other hand, must be divided into a larger number of sequential memory operations. One of the aspects that make GPU programming still quite complex is that, in most cases, the hierarchy of levels of memory, in particular the shared memory, has to be

managed explicitly by the programmer. In return, this explicit management is often an opportunity for further optimizations and better performances.

### 6.2.4 GPU-Based Parallel Implementation of the Single-Signal Algorithm

In the work presented here we did not produce a parallel implementation of the single-signal algorithm, but we relied on the results reported in the literature, instead.

For the parallelization of (single-signal) growing self-organizing network algorithms, a very common approach is applying the well-known *map-reduce* pattern, which can be easily parallelized into a two-step method, to the dominant *Find Winners* phase. In the first step of the *map-reduce* approach, i.e. the *map* operation, the distance from each unit to the input signal is computed in parallel. In the second step, i.e. the *reduce* operation, the set of previously computed distances is iteratively reduced by comparing subsets in parallel, until the  $k$  shortest distances are found. In passing, Buck et al. describe GPU reductions in more detail in the context of the Brook programming language [18], while Harris does it in [19] for the CUDA language. The map-reduce pattern has been studied in general [20] and applied to the search of  $k$  nearest neighbors ( $k$ -NN) [21]. More specifically this approach has been used for the parallelization of the GNG algorithm (see [5] and [4]) and of the Parameter-Less SOM (see [7]).

The *map-reduce* approach, however, implies a one-to-one correspondence between network units and GPU threads in the *map* phase, which becomes even lower in the *reduce* phase. This fact becomes a substantial limitation for the parallelization of growing self-organizing networks, which usually start with a very small number of units and grow progressively during the execution. As reported (see [5]), unless the network contains at least 500–1000 units, the sequential execution on a CPU can be faster than the parallel one. To cope with this problem, a hybrid technique has been proposed (see [5] and [4]): switching the execution from CPU to GPU only when the network is sufficiently large and the latter hardware is expected to perform better. Nevertheless, even with this hybrid solution, the maximum level of parallelization that can be attained is bound to the number of units in the network.

### 6.2.5 GPU-Based Parallel Implementation of the Multi-Signal Variant

For the GPU-based parallel implementation of the algorithm, the main advantage of the multi-signal variant is that the level of parallelism is bound only by the number of signals submitted to the network at each iteration. Furthermore this same level of parallelism can be maintained across entire kernels, since no reduction takes place.



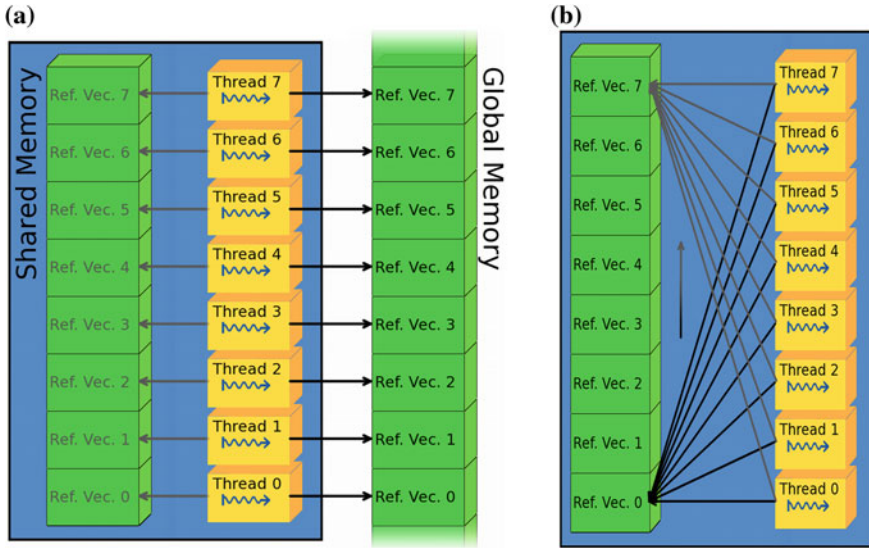


**Fig. 6.5** The two steps of the Find Winners phase in the parallel implementation. **a** Parallel load, **b** Sequential scan

The only limitation of this variant comes from the collisions that can occur during the *Update* phase, as explained in Sect. 6.2.2. Nevertheless, if the parallel implementation focuses on the dominant *Find Winners* phase, there is in practice no upper limit for the level of parallelism, beyond that of the hardware.

In the *kernel* that has been realized for the *Find Winners* phase, each thread is assigned to an input signal. The execution is divided in two steps (see Fig. 6.5): first, all threads in a block load a contiguous batch of reference vectors in the shared memory with a *coalesced* access; second, all threads compute the distances from the reference vectors to the signal through a sequential scan of the shared memory, in which all threads read the same reference vector in sync. From the point of view of GPU-based parallelization, this allows harnessing the faster and smaller *shared memory* in order to accelerate the access to the *global memory*, i.e. where the whole set of reference vectors is stored.

## 6.3 Experimental Validation

### 6.3.1 Methods of Comparison

All the experiments described in this section have been performed with the SOAM algorithm, in four different implementations (see below), applied to the same tasks

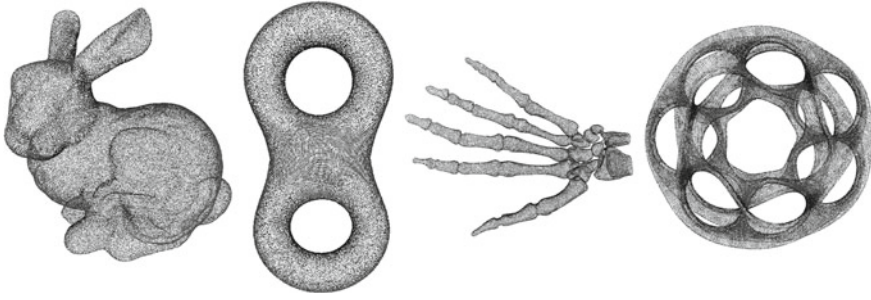


**Fig. 6.6** The four point-clouds used in the test phase

of surface reconstruction from point clouds. In each experiment, the point cloud was taken from a triangular mesh and sampled with uniform probability distribution  $P(\xi)$ .

Four different meshes have been used, each having different *topological* and *geometrical complexity*. More precisely, we consider two measures, one for each type of complexity: the *genus* of the surface [22], i.e. the number of holes enclosed by it, and the *local feature size* (LFS), defined in each point  $x$  of the surface as the minimal distance to the medial axis [23]. In this perspective, a ‘simple’ mesh has genus zero or very low and almost constant LFS values, while a ‘complex’ mesh has higher genus and LFS values that vary widely across different areas.

The four meshes used in the experiments are well-known benchmarks for surface reconstruction (Fig. 6.6):

- *Stanford Bunny*. It has genus 0 and some non-negligible variations in the LFS values that make it non-trivial.
- *Eight* (also called *double torus*). It has genus 2 and relatively constant LFS values almost everywhere.
- *Skeleton Hand*. It has genus 5 and widely variable LFS values, that in many areas, e.g. close to the wrist, become considerably low.
- *Heptoroid*. It has genus 22, and low and variable LFS values over the surface.

Obviously, there is no *a priori* guarantee that a parallel algorithm should be faster than a highly-optimized sequential one. Therefore we chose to implement also a single-signal variant of the algorithm in which the crucial *Find Winners* phase is improved through the use of a *hash indexing* method, similar to that used in molecular dynamics [24].

The hash index is constructed by defining a grid of cubes of fixed size inside an axis-parallel bounding box that contains all the input signals in the input space. The hash index of both signals and reference vectors, which live in the same space, is obtained from the 3D coordinates. Whenever an input signal is selected, the search for the reference vectors of the winner and the second nearest units is first performed on the same cube where the input signal resides, together with its 26 adjacent cubes. If this search fails, the exhaustive search is performed instead. Even if this method is

slightly approximate, in that in a few extreme cases it may produce different results from the exhaustive search, it yields a substantial speed-up, as will be discussed in Sect. 6.3.3. In addition, being a hash method, the maintenance of the index, which is performed in the *Update* phase, does not affect performances in a significant way.

Four different implementations of the SOAM algorithm have been used for the experiments:

- *Single-signal*. A reference implementation of the single-signal SOAM algorithm in C.
- *Indexed*. The same single-signal algorithm, but using an hash index for the *Find Winners* phase.
- *Multi-signal*. A reference implementation in C of the multi-signal variant of the algorithm, as described in Sects. 6.2.2 and 6.2.5 but without any actual parallelization, in terms of execution.
- *GPU-Based*. An implementation in C and NVIDIA C/CUDA of the multi-signal variant of the algorithm, with actual hardware parallelization.

The tests have been performed on a Dell Precision T3400 workstation, with a NVidia GeForce GT 440, i.e. an entry-level GPU based on the *Fermi* architecture. The operating system was MS Windows Vista *Business* SP2 and all the programs have been compiled with MS Visual C++ Express 2010, with the CUDA SDK version 4.0.

All the shared input parameters have been set to the same values for all the tests for the four different implementations, while implementation-specific parameters, such as the level of parallelism or the index cube size, have been tuned specifically for maximum performances. Among the shared input parameters, only the crucial *insertion threshold* has been tuned for each mesh, for the reasons described in [1], while every other parameter value has been kept constant for all the four meshes.

In order to avoid discarding an excessive number of signals in the *Update* phase, in all parallel implementations the level of parallelism  $m$  at each iteration, i.e. the number of signals processed in the iteration, is set to the minimum power of two greater than the current number of units in the network. The maximum level of parallelism has been set to 8192.

Tables 6.1, 6.2, 6.3 and 6.4, at the end of this section, show the numerical results obtained from the experiments. As it can be seen, for each input mesh, each different implementation reaches a final configuration which can be either different or very different, e.g. for the skeleton hand, in terms of number of units and connections. Note that multi-signal and GPU-based implementations reach exactly the same final configuration, since they are meant to replicate the same behavior by design.

As expected, there are substantial differences also for execution times. In the tables these are measured as *total time to convergence* and *time per signal*, and the detail figures are reported for each of the three phases. Time per signal is a measure of the raw performances that can be obtained with each implementation, while time to convergence is the combined result of the implementation *and* the different behavior that each implementation induces, as it will be explained in the next sections.

**Table 6.1** Execution time and statistics on the Stanford Bunny data-set

Algorithm version	Single-signal	Indexed	Multi-signal	GPU-based
<i>Network configuration at convergence</i>				
Iterations	620,000	616,000	1,296	1,296
Signals	620,000	616,000	580,656	580,656
Discarded signals	0	0	319,054	319,054
Units	330	332	347	347
Connections	984	990	1,035	1,035
<i>Time to convergence</i>				
Total time	4.9530	3.369	3.893	2.059
Sample	0.460	0.048	0.009	0.016
Find winners	2.610	1.233	2.448	0.699
Update	1.883	2.088	1.436	1.344
<i>Time per signal</i>				
Time per signal	$7.9887 \times 10^{-06}$	$5.4692 \times 10^{-06}$	$6.7045 \times 10^{-06}$	$3.5460 \times 10^{-06}$
Find winners	$4.2097 \times 10^{-06}$	$2.0016 \times 10^{-06}$	$4.2159 \times 10^{-06}$	$1.2038 \times 10^{-06}$

**Table 6.2** Execution time and statistics on the Eight data-set

Algorithm version	Single-signal	Indexed	Multi-signal	GPU-based
<i>Network configuration at convergence</i>				
Iterations	1,100,000	1,100,000	1,128	1,128
Signals	1,100,000	1,100,000	1,100,110	1,100,110
Discarded signals	0	0	562,277	562,277
Units	656	649	658	658
Connections	1,974	1,953	1,980	1,980
<i>Time to convergence</i>				
Total time	12.3540	5.5690	11.6070	3.8690
Sample	0.0150	0.0480	0.0620	0.1410
Find winners	8.8600	2.8220	8.5060	0.7650
Update	3.4790	2.6990	3.0390	2.9630
<i>Time per signal</i>				
Time per signal	$1.1231 \times 10^{-05}$	$5.0627 \times 10^{-06}$	$1.0551 \times 10^{-05}$	$3.5169 \times 10^{-06}$
Find winners	$8.0545 \times 10^{-06}$	$2.5655 \times 10^{-06}$	$7.7320 \times 10^{-06}$	$6.9539 \times 10^{-07}$

### 6.3.2 Behavior of the Multi-Signal Algorithm

The first five lines of Tables 6.1, 6.2, 6.3 and 6.4, highlight an aspect that is worth some further discussion, in particular for the *Single-signal* and the *Multi-signal* implementations.

Regardless of the hardware parallelization, the *Multi-signal* variant always needs a substantially lower number of input signals than the *Single-signal* one to converge. This difference becomes even more evident if the discarded signals are not counted for, approaching a ratio of one to four as the mesh becomes more complex.

**Table 6.3** Execution time and statistics on the Hand data-set

Algorithm version	Single-signal	Indexed	Multi-signal	GPU-based
<i>Network configuration at convergence</i>				
Iterations	202,988,000	213,800,000	10.264	10.264
Signals	202,988,000	213,800,000	81.092.912	81.092.912
Discarded signals	0	0	33.432.622	33.432.622
Units	5,669	5,766	8.884	8.884
Connections	17,037	17,328	26.688	26.688
<i>Time to convergence</i>				
Total time	18, 548.4937	5, 337.2451	12, 422.3738	872.0250
Sample	9.4050	35.9820	8.6120	8.0480
Find winners	17, 763.1367	4, 127.8511	11, 789.8398	241.1750
Update	775.9520	1, 173.4120	623.9220	622.8020
<i>Time per signal</i>				
Time per signal	$9.1377 \times 10^{-05}$	$2.4964 \times 10^{-05}$	$1.5319 \times 10^{-04}$	$1.0753 \times 10^{-05}$
Find winners	$8.7508 \times 10^{-05}$	$1.9307 \times 10^{-05}$	$1.4539 \times 10^{-04}$	$2.9741 \times 10^{-06}$

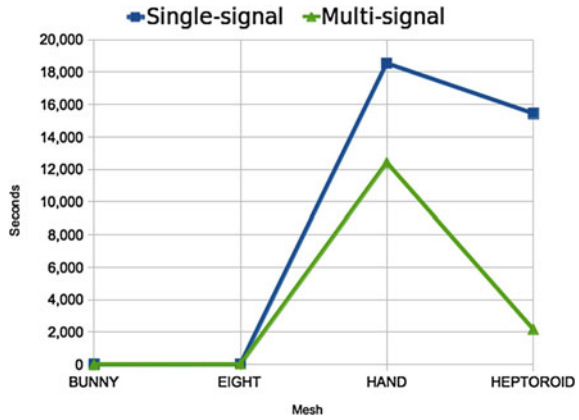
**Table 6.4** Execution time and statistics on the Heptoroid data-set

Algorithm version	Single-signal	Indexed	Multi-signal	GPU-based
<i>Network configuration at convergence</i>				
Iterations	20,714,000	23,684,000	1,244	1,244
Signals	20,714,000	23,684,000	7,683,554	7,683,554
Discarded signals	0	0	2,262,969	2,262,969
Units	14,183	13,937	15,638	15,638
Connections	42,675	41,937	47,040	47,040
<i>Time to convergence</i>				
Total time	15, 449.2950	950.0250	2, 172.8009	119.6530
Sample	6.9570	3.4550	0.8010	0.5630
Find winners	15, 294.3330	780.5370	2, 089.6169	34.2640
Update	148.0050	166.0330	82.3830	84.8260
<i>Time per signal</i>				
Time per signal	$7.4584 \times 10^{-04}$	$4.0113 \times 10^{-05}$	$2.8279 \times 10^{-04}$	$1.5573 \times 10^{-05}$
Find winners	$7.3836 \times 10^{-04}$	$3.2956 \times 10^{-05}$	$2.7196 \times 10^{-04}$	$4.4594 \times 10^{-06}$

The decrease in the number of signals to convergence is attained despite the growth in the number of units and connections reached in the final configuration.

Figure 6.7 compares the times to convergence of the *Single-signal* and *Multi-signal* implementations. The performances of *Multi-signal* implementation are always better than its *Single-signal* counterpart, a difference that becomes more substantial as the complexity of the mesh increases. Overall, this means that the extra load due to the increase in the number of both units and connections is outbalanced by the decrease in the number of signals needed to reach convergence.

Fig. 6.7 Time to convergence of the Single-signal and Multi-signal implementations



In a possible explanation, the multi-signal variant has a better inherently distributed behavior than the original variant. In fact, in each iteration of the multi-signal variant, a randomly scattered set of units is updated ‘simultaneously’, whereas in the single-signal variant only the winner unit and its direct neighbors are updated. Apparently, the more distributed update leads to a more effective use of the input signals, yielding faster convergence. This aspect, however, requires further investigation.

### 6.3.3 GPU-Based Implementation Performances

Figure 6.8 shows a summary of the total times to convergence for the *Single-signal*, *Indexed* and *GPU-based* implementations respectively, for the two most complex meshes, with detail figure per each phase. Remarkably, in the *GPU-based* implementation, the *Find Winners* phase ceases to be dominant, and the *Update* phase becomes the most time-consuming. This means that in this implementation any further optimization of the *Find Winners* phase is less relevant unless the execution of the *Update* phase is sped up in turn.

More in detail, Fig. 6.9a shows the average times per signal spent in the *Find Winners* phase for each of the three implementations. Clearly, these times grow as the number of the units in the network becomes larger. Figure 6.9b compares the speed-up factors in average time per signal for the *Indexed* and *GPU-based* implementations with respect to the *Single-signal* one. As expected, these factors also grow with the number of units in the network, since the hash index in the *Indexed* implementation becomes more effective, while an higher level of parallelism can be achieved in the *GPU-based* implementation. Overall, the speed-up factor for the GPU-based implementation reaches 165x on the *Heptoroid* mesh.

Figure 6.10a shows the total times to convergence. These results show how the performances of the SOAM algorithm depend on the variation in the LFS values

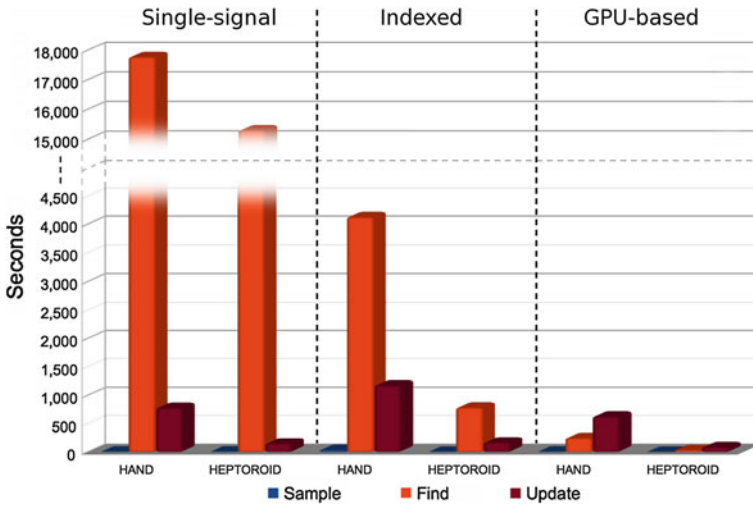


Fig. 6.8 Single-phase time to convergence for the two more complex meshes in the test set

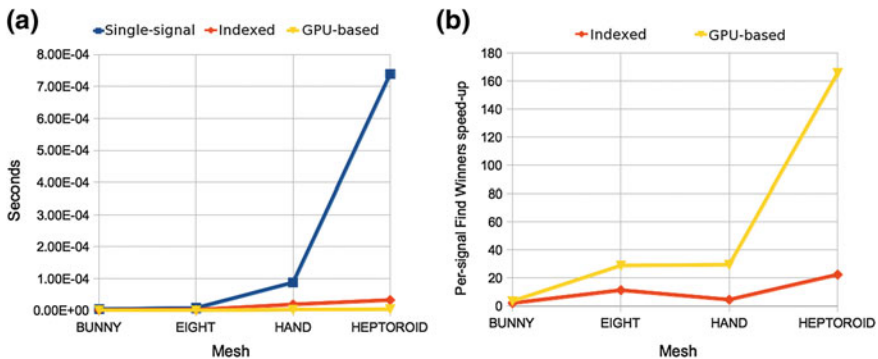
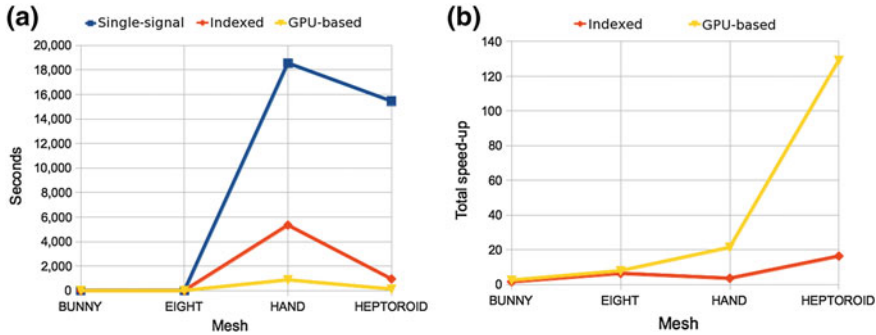


Fig. 6.9 Per-signal performances. **a** Times per signal in the Find Winner phase for the three implementations. **b** Speed-up factors for the Find Winners phase time per signal compared to the Single-signal implementation

(see Sect. 6.3.1): in fact, the skeleton hand always requires the longest time to convergence, regardless of the implementation. Figure 6.10b shows the speed-up factors for the time to convergence, for the *Indexed* and *GPU-based* implementations, again with respect to the *Single-signal* one. These factors grow with the number of units in the network, and are the combined results of the implementation and of the behavior induced.

For all input meshes, the total times to convergence for the *GPU-based* implementation are much lower than the ones for the *Single-signal* implementation. Speed-ups vary from 2.5x (bunny) to 129x (heptoroid), as the complexity of the mesh increases and the size of the reconstructed network grows. In particular, the results obtained



**Fig. 6.10** Global performances. **a** Times to convergence for the three implementations. **b** Speed-up factors for the times to convergence compared to the Single-signal implementation

with the *Stanford Bunny*, given in Table 6.1, show non negligible speed-up factors in both the total time to convergence (2.5x) and the time per signal (3.5x), despite that the network contains only 330–347 units at most.

This result is particularly relevant if compared to other GPU-based parallel implementations of growing self-organizing networks (see for example [5]), for which it is reported that the GPU execution produces noticeable speed-ups only when the networks contain no less than 500–1000 units.

The *Indexed* implementation of the algorithm also obtains noticeable speed-ups on all test cases. Nonetheless, as shown in Fig. 6.8, the *Find Winners* phase is still dominant, although with *Stanford bunny* and *Eight* the *Update* times become comparable.

## 6.4 Conclusions and Future Developments

In this chapter we examined the parallelization of growing self-organizing networks by proposing a multi-signal variant of the original algorithm adopted, in order to increase its parallel scalability.

In particular, the experiments show that this multi-signal variant adapts naturally to the GPU architecture in that, besides the advantages deriving from the careful management of hierarchical memory through perfectly coalesced memory accesses, it leads to a better usage of the high number of cores by allowing very high numbers of concurrent threads.

A further interesting, and somehow unexpected, result of the experiments is that, hardware parallelization apart, the overall behavior of the multi-signal variant is significantly different from the original, single-signal one. The multi-signal variant of the algorithm, in fact, seems to better deal with complex meshes, by requiring a smaller number of signals in order to reach network convergence. This aspect needs to be further investigated, possibly with more specific and extensive experiments.



The parallelization described in this chapter is limited to the dominant *Find Winners* phase and, according to the experimental results, can successfully make it less time-consuming than the *Update* phase. This means that future developments of the strategy proposed should aim to the parallelization of the *Update* phase as well, in order to further improve on performances. This requires some care however, as the *collisions* among threads trying to update the data structures involved, must be managed with care.

## References

1. Piasra, M.: Self-organizing adaptive map: autonomous learning of curves and surfaces from point samples. *Neural Netw.* **41**, 96–112 (2012)
2. Lawrence, R., Almasi, G., Rushmeier, H.: A scalable parallel algorithm for self-organizing maps with applications to sparse data mining problems. *Data Min. Knowl. Disc.* **3**, 171–195 (1999)
3. Kohonen, T.: *Self-Organizing Maps*. Springer series in information sciences, vol. 30. Springer, Berlin (2001)
4. Orts, S., Garcia-Rodriguez, J., Viejo, D., Cazorla, M., Morell, V.: Gpgpu implementation of growing neural gas: application to 3d scene reconstruction. *J. Parallel Distrib. Comput.* **72**(10), 1361–1372 (2012)
5. García-Rodríguez, J., Angelopoulou, A., Morell, V., Orts, S., Psarrou, A., García-Chamizo, J.: Fast image representation with gpu-based growing neural gas. *Adv. Comput. Intell., Lect. Notes Comput. Sci* **6692**, 58–65 (2011)
6. Luo, Z., Liu, H., Wu, X.: Artificial neural network computation on graphic process unit. In: *Proceedings of the IEEE International Joint Conference on Neural Networks, IJCNN'05. IEEE 2005*, vol. 1, pp. 622–626 (2005)
7. Campbell, A., Berglund, E., Streit, A.: Graphics hardware implementation of the parameter-less self-organising map. In: *Intelligent Data Engineering and Automated Learning-IDEAL 2005*, pp. 5–14 (2005)
8. Owens, J., Luebke, D., Govindaraju, N., Harris, M., Krüger, J., Lefohn, A., Purcell, T.: A survey of general-purpose computation on graphics hardware. *Comput. Graphics Forum* **26**, 80–113 (2007) (Wiley Online Library)
9. Fritzke, B.: *A growing neural gas network learns topologies*. In: *Advances in Neural Information Processing Systems 7*, MIT Press (1995)
10. Marsland, S., Shapiro, J., Nehmzow, U.: A self-organising network that grows when required. *Neural Netw.* **15**, 1041–1058 (2002)
11. Martinetz, T., Schulten, K.: Topology representing networks. *Neural Netw.* **7**, 507–522 (1994)
12. Owens, J., Houston, M., Luebke, D., Green, S., Stone, J., Phillips, J.: Gpu computing. *Proc. IEEE* **96**, 879–899 (2008)
13. McCool, M.: Data-parallel programming on the cell be and the gpu using the rapidmind development platform. In: *GSPx Multicore Applications Conference*. vol. 9. (2006)
14. Papakipos, M.: *The Peakstream Platform: High-Productivity Software Development for Multi-Core Processors*. PeakStream Inc., Redwood City (2007)
15. NVIDIA Corporation: *CUDA C programming guide, version 4.0*. Santa Clara (2011)
16. Hensley, J.: AMD CTM overview. In: *ACM SIGGRAPH 2007 courses*, p. 7. ACM, New York (2007)
17. Stone, J., Gohara, D., Shi, G.: Opencl: a parallel programming standard for heterogeneous computing systems. *Comput. Sci. Eng.* **12**, 66 (2010)
18. Buck, I., Foley, T., Horn, D., Sugerman, J., Fatahalian, K., Houston, M., Hanrahan, P.: Brook for gpus: stream computing on graphics hardware. *ACM Trans. Graph.* **23**, 777–786 (2004)

19. Harris, M.: Optimizing parallel reduction in cuda. CUDA SDK Whitepaper (2007)
20. Liu, S., Flach, P., Cristianini, N.: Generic multiplicative methods for implementing machine learning algorithms on mapreduce. Arxiv, preprint arXiv:1111.2111 (2011)
21. Zhang, C., Li, F., Jests, J.: Efficient parallel knn joins for large data in mapreduce. In: Proceedings of 15th International Conference on Extending Database Technology (EDBT 2012). (2012)
22. Edelsbrunner, H.: GGeometry and topology for mesh generation. Cambridge Monographs on Applied and Computational Mathematics, vol. 7. Cambridge University Press, Cambridge (2001)
23. Amenta, N., Bern, M.: Surface reconstruction by voronoi filtering. *Discrete Comput. Geom.* **22**, 481–504 (1999)
24. Hockney, R.W., Eastwood, J.W.: *Computer Simulation Using Particles*. Taylor & Francis Inc., Bristol (1988)